

Vibration of Infinite Timoshenko Beam on Pasternak Foundation under Vehicular Load

Weili LUO and Yong XIA*

Department of Civil and Environmental Engineering, The Hong Kong Polytechnic University,
Kowloon, Hong Kong

*Corresponding author, email: ceyxia@polyu.edu.hk

Abstract: The vibration of beams on foundations under a vehicular load has attracted wide attention for decades. The problem has numerous applications in several fields such as highway structures. However, most of analytical or semi-analytical studies simplify the vehicular load as a concentrated point or distributed line load with the constant or harmonically varying amplitude, and neglect the presence of the vehicle and the road irregularity. This paper carries out an analytical study of vibration on an infinite Pasternak supported Timoshenko beam under vehicular load, which is obtained by the passage of a quarter car on a road with harmonic surface irregularity. The governing equations of motion are derived based on the Hamilton principle and Timoshenko beam theory, and then are solved in the frequency-wavenumber domain with a moving coordinate system. The analytical solutions are expressed in a general form of Cauchy's residue theorem. The results are validated by the case of an Euler-Bernoulli beam on a Winkler foundation, which is a specific case of the current system and has an explicit form of solution. Finally, a numerical example is employed to investigate the influence of properties of the beam

(the radius of gyration and the shear rigidity) and the foundation (the shear viscosity, rocking and normal stiffness) on the deflected shape, maximum displacement, critical frequency, and critical velocity of the system.

Key words: Moving load, Timoshenko beam, Pasternak foundation, analytical solution

1. INTRODUCTION

Super-high-speed and super-high-capacity vehicles nowadays are increasingly adopted as land transportation carriers. Their safety becomes a public concern when the vehicle speed exceeds the critical velocity of the road-subsoil system or when the load frequency approaches the critical frequency of the system (Metrikine and Dieterman 1997; Verichev and Metrikine 2002; Wolfert *et al.* 1998). In this regard, the model of beams on elastic or viscoelastic foundations has drawn wide attentions, in which the beam and foundation are reasonable idealizations of the road and the subsoil, respectively.

In the past decades, analytical solutions to vibration of beams on elastic or viscoelastic foundations were presented. Among them, Kenney (1954) first derived a closed-form solution to the Winkler foundation supported Euler-Bernoulli (EB) beam vibrations when subjected to a concentrated load moving at a constant velocity. Later, Mathews (1958) and Frýba (1999) extended Kenney's solution to account for harmonic load and Kelvin foundation, respectively. Other closed-form solutions include a solution of an EB beam on a Winkler foundation under a

harmonic line load with (Sun 2003) or without velocity (Sun 2001); a solution of an EB beam on a Kelvin foundation under a moving concentrated load (Sun 2002); a solution to a viscoelastically supported Timoshenko beam under a harmonic line load (Luo, *et al.* 2016). If the model is more complicated, the analytical solution can only be written in a form of Cauchy's residue theorem. This is because the characteristic equations of most beam-foundation systems are polynomials of degree four/five, and their roots usually cannot be expressed using elementary functions (Luo, *et al.* 2015). Representative works, to name a few, contain the steady-state vibration of a Timoshenko beam on a Pasternak foundation under a harmonic moving load (Kargarnovin and Younesian 2004); the dynamic behavior of a laminated composite beam supported by a generalized Pasternak-type viscoelastic foundation when subjected to a moving oscillator with two degrees of freedom (DOFs) (Ahmadian *et al.* 2008); and the steady-state vibration of a Timoshenko beam made of a laminated composite on a Pasternak viscoelastic foundation under a concentrated harmonic moving load (Rezvani and Khorramabadi 2009).

Semi-analytical approaches are also used to deal with the complicated model, which avoid identification of the roots and directly solve the integral representation of the beam deflection using numerical algorithms. One may refer to the use of inverse fast Fourier transform for an arbitrary load induced vibration of a Timoshenko beam on a hysteretically damped elastic foundation (Luo *et al.* 2015) and line loads induced vibrations of a viscoelastically supported EB beam (Kim and Roesset 2003), Rayleigh beam-column (Kim 2005), and shear beam-column (Kim and Cho 2006). One may also refer to the use of Durbin's inverse Laplace transform for time-dependent loads induced vibration of an EB beam on a Pasternak foundation (Çalım 2009).

However, most of these studies neglect the vehicle dynamic system and surface irregularity, and thus simplify the vehicular load as an idealized form, such as a concentrated point or a distributed line load with constant or harmonic amplitude. This paper intends to analytically investigate a more realistic vehicular load induced vibration of an infinite Timoshenko beam on a Pasternak foundation. This load is obtained from a quarter car travelling on a road with harmonic surface irregularity. The road is represented by a Timoshenko beam rather than EB beam because the former is able to take account of shear deformation and rotational inertia. A Pasternak foundation has extra viscous layer and thus is more realistic to represent the subsoil, as by compared with the Winkler or Kelvin counterpart. The governing equations of motion of the beam-foundation-vehicle system are derived using the Hamilton principle and Timoshenko theory, and are subsequently reduced to algebraic equations by assuming that the deflection and rotation of beam are harmonic with respect to moving space and time. The deflection of the beam are obtained by using inverse Fourier transform together with Cauchy's residue theorem. The solution is validated by comparing with the closed-form solutions of an EB beam on a Winkler foundation. The influences of the beam and the foundation's properties on the deflected shape, maximum deflection, critical frequency, and critical velocity are investigated through a numerical example.

2. PROBLEM FORMULATION

Figure 1 shows a beam-foundation-vehicle system with the following assumptions: (a) the beam is infinitely long and homogenous along both thickness and axial directions; (b) the extra shear

layer accounts for rocking stiffness, shear viscosity, and damping; and (c) the vehicle is simplified as a quarter car model with 2 DOFs, and travels at a constant velocity.

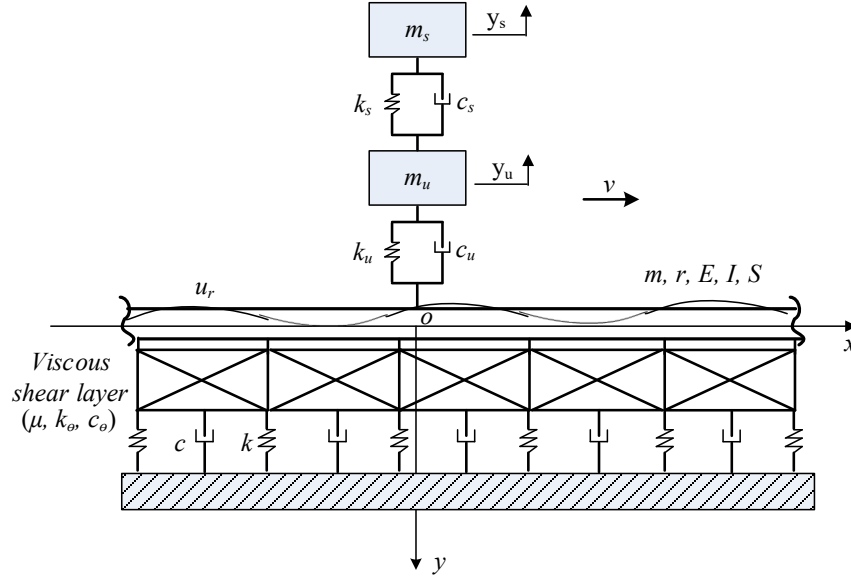


Figure 1. An infinite Timoshenko beam on a Pasternak foundation under a vehicular load

By using Hamilton principle and Timoshenko beam theory, the governing equations of motion of this system can be obtained as follows (Ahmadian *et al.* 2008):

$$m\ddot{w}(x,t) + S[\theta'(x,t) - w''(x,t)] - P_f(x,t) = q(t)\delta(x - vt) \quad (1a)$$

$$EI\theta''(x,t) + S[w'(x,t) - \theta(x,t)] + M_f(x,t) = mr^2\ddot{\theta}(x,t) \quad (1b)$$

where $w(x,t)$ and $\theta(x,t)$ are the deflection and rotation of the beam, respectively; m is the mass of the beam per unit length; E is the Young's modulus; I is the cross sectional moment of inertia; S and r are the shear rigidity and the radius of gyration of the beam, respectively; the dot over a variable denotes the differentiation with respect to time; the prime of a variable denotes the

differentiation with respect to space; δ is the Dirac function; and v is the vehicle velocity; P_f and M_f are, respectively, the foundation simulated force and moment per unit length of the beam given as follows (Ahmadian *et al.* 2008):

$$P_f(x, t) = -kw(x, t) - c\dot{w}(x, t) + \mu\dot{w}''(x, t) \quad (2)$$

$$M_f(x, t) = -k_\theta\theta(x, t) - c_\theta\dot{\theta}(x, t) \quad (3)$$

where k , c , k_θ , c_θ , and μ are normal stiffness, normal damping, rocking stiffness, rocking damping, and shear viscosity coefficients of the foundation, respectively; and the vehicular load $q(t)$ is given by (Lombaert, *et al.* 2000):

$$q(t) = k_u(y_u - u_r - w) + c_u(\dot{y}_u - \dot{u}_r - \dot{w}) \quad (4)$$

where u_r is the surface irregularity; c_u and k_u are damping and stiffness of vehicle unsprung components, respectively; and y_u is vertical displacement of vehicle unsprung components, which is determined by the following two governing equations of motion of a quarter car model (Cebon 1999):

$$m_s\ddot{y}_s + c_s(\dot{y}_s - \dot{y}_u) + k_s(y_u - y_s) = 0 \quad (5a)$$

$$m_u\ddot{y}_u + c_u(\dot{y}_s - \dot{u}_r) + c_s(\dot{y}_u - \dot{y}_s) + k_u(y_s - u_r) + k_s(y_u - y_s) = 0 \quad (5b)$$

where subscripts s and u denote sprung and unsprung components of the car model, respectively.

Eqn 4 indicates that the computation of vehicular load $q(t)$ is a coupled problem, and thus requires simultaneously solving Eqns 1 and 5, particularly for the vehicle-bridge interaction problem (Gao *et al.* 2015; Yin *et al.* 2016). However, for the research of interest in this paper,

the vibration of the vehicle-road system, this coupled effect can be ignored because the stiffness of the road is much higher than that of the vehicle (Hao and Ang 1998; Hunt 1991; Ju 2009; Lombaert *et al.* 2000). Consequently, the items (w and \dot{w}) are removed from Eqn 4.

Since the length of the beam is assumed to be infinite, the deflection, shear force, and moment of the beam vanish on both sides of infinite boundary ($\pm\infty$), i.e.:

$$w(x,t)=0, \quad w'(x,t)=0, \quad \theta(x,t)=0, \quad \theta'(x,t)=0 \quad (6)$$

3. ANALYTICAL SOLUTION

A moving coordinate system attached to the vehicle is first introduced:

$$x_1 = x - vt, \quad w_1 = w, \quad \theta_1 = \theta \quad (7)$$

where subscript “₁” denotes the variable in the moving coordinate system.

According to the chain rule of differentiation, the following equations are derived:

$$\begin{aligned} \eta'(x,t) &= \eta'_1(x_1,t) \\ \eta''(x,t) &= \eta''_1(x_1,t) \\ \dot{\eta}(x,t) &= \dot{\eta}_1(x_1,t) - v\eta'_1(x_1,t) \\ \ddot{\eta}(x,t) &= \ddot{\eta}_1(x_1,t) - 2v\dot{\eta}'_1(x_1,t) + v^2\eta''_1(x_1,t) \end{aligned} \quad (8)$$

where η represents w or θ .

140 By substituting Eqns 7 and 8 into Eqn 1, the governing equations of motion of the system can be
 141 rewritten as follows:

$$142 \quad m(\ddot{w}_1 - 2v\dot{w}_1' + v^2 w_1'') + S(\theta_1' - w_1'') + k w_1 + c(\dot{w}_1 - v w_1') - \mu(\dot{w}_1'' - v w_1''') = q \delta \quad (9a)$$

$$143 \quad EI\theta_1'' + S(w_1' - \theta_1) - k_\theta \theta_1 - c_\theta(\dot{\theta}_1 - v\theta_1') = mr^2(\ddot{\theta}_1 - 2v\dot{\theta}_1' + v^2 \theta_1'') \quad (9b)$$

144 where x_1 and t are omitted for brevity.

145

146 The road irregularity is assumed to be spatially harmonic with wavenumber k_r (Lombaert *et al.*
 147 2000):

$$148 \quad u_r = U_r \exp(ik_r x) \quad (10)$$

149 where U_r is amplitude of the road irregularity. By using $x = vt$ and $\omega = vk_r$ where ω is the load
 150 circular frequency, Eqn 10 can be written in a temporally harmonic form:

$$151 \quad u_r = U_r \exp(i\omega t) \quad (11)$$

152 The resulting vehicular load is also harmonic, i.e., $q(t) = Q \exp(i\omega t)$, where Q is amplitude of the
 153 vehicular load.

154

155 Assume $w_1(t) = W_1 \exp(-ik_x x) \exp(i\omega t)$ and $\theta_1(t) = \Theta_1 \exp(-ik_x x) \exp(i\omega t)$ where W_1 and Θ_1 are,
 156 respectively, amplitudes of the beam deflection and rotation in the moving coordinate system,
 157 and k_x is the wavenumber of moving space x_1 . Substituting $w_1(t)$ and $\theta_1(t)$ into Eqn 9, one can
 158 obtain the governing equations of motion of the system in the frequency–wavenumber ($\omega-k_x$)
 159 domain:

$$-m(\omega - k_x v)^2 W_1 + S(ik_x \Theta_1 + k_x^2 W_1) + kW_1 + c(i\omega W_1 - vk_x W_1) - \mu(-i\omega k_x^2 W_1 + ivk_x^3 W_1) = Q \quad (12a)$$

$$-EI k_x^2 \Theta_1 + S(ik_x W_1 - \Theta_1) - k_\theta \Theta_1 - c_\theta(i\omega \Theta_1 - vk_x \Theta_1) = -mr^2(\omega - vk_x)^2 \Theta_1 \quad (12b)$$

162

163

164 Similarly, the governing equations of motion of the vehicle in the frequency domain can be
165 rewritten in a matrix form (Hao and Ang 1998):

$$\begin{bmatrix} A_{ss} & A_{su} \\ A_{us} & A_{uu} \end{bmatrix} \begin{Bmatrix} Y_s \\ Y_u \end{Bmatrix} = \begin{bmatrix} 0 \\ BU_r \end{bmatrix} \quad (13)$$

167 where Y_s and Y_u are amplitudes of y_s and y_u , respectively; and A and B are defined as follows:

$$A_{ss} = -\Omega^2 + 2i\xi_s \Omega + 1 \quad (14a)$$

$$A_{su} = A_{us} = -(2i\xi_s \Omega + 1) \quad (14b)$$

$$A_{uu} = -\zeta \Omega^2 + 2i(\zeta ab + 1)\xi_s \Omega + (\zeta a^2 + 1) \quad (14c)$$

$$B = 2i\zeta ab \xi_s \Omega + \zeta a^2 \quad (14d)$$

172 where $\omega_j = \sqrt{k_j/m_j}$ is the vehicle natural frequency ($j = s$ or u); $\xi_j = c_j/2\sqrt{m_j k_j}$ is the vehicle
173 damping ratio ($j = s$ or u); and Ω , ζ , a , and b are defined as $\Omega = \omega/\omega_s$, $\zeta = m_u/m_s$, $a = \omega_u/\omega_s$, and b
174 $= \xi_u/\xi_s$, respectively. The vehicular load in the frequency domain is also given by (Hao and Ang
175 1998):

$$Q = \frac{m_s \omega^2 B}{\Delta} (A_{su} - \zeta A_{ss}) U_r \quad (15)$$

177 where $\Delta = A_{ss}A_{uu} - A_{su}A_{us}$ is the determinant of the coefficient matrix in Eqn (13).

178

179 Eqn 12 consists of two linear equations of Θ_1 and W_1 . By eliminating Θ_1 , one obtains the beam
 180 deflection moving with the load in the wavenumber-frequency domain:

$$181 \quad W_1(k_x, \omega) = \frac{Q}{-m(\omega - k_x v)^2 + M + S k_x^2 + k + i c(\omega - v k_x) + i \mu(\omega k_x^2 - v k_x^3)} \quad (16)$$

$$182 \quad \text{where } M = \frac{-S^2 k_x^2}{-m r^2(\omega - k_x v)^2 + E I k_x^2 + S + k_\theta + i c_\theta(\omega - v k_x)}.$$

183

184 Combining the coefficients at the same order of k_x , Eqn 16 can then be rearranged as follows:

$$185 \quad W_1(k_x, \omega) = \frac{(C_1 k_x^2 + C_2 k_x + C_3) Q}{C_4 k_x^5 + C_5 k_x^4 + C_6 k_x^3 + C_7 k_x^2 + C_8 k_x + C_9} \quad (17)$$

186 where C_1 to C_9 are coefficients given in Appendix; and the denominator is usually termed as the
 187 characteristic equation.

188

189 Applying an inverse Fourier transform to Eqn 17 yields the following beam deflection in a
 190 general integral form:

$$191 \quad w_1(x_1, \omega) = \frac{1}{2\pi} \int_{-\infty}^{+\infty} \frac{(C_1 k_x^2 + C_2 k_x + C_3) Q \exp(-i k_x x)}{i C_4 k_x^5 + C_5 k_x^4 + C_6 k_x^3 + C_7 k_x^2 + C_8 k_x + C_9} dk_x \quad (18)$$

192

193 By employing Cauchy's residue theorem, the analytical solution of Eqn 18 is given as follows:

$$w_1(x_1, \omega) = \begin{cases} +\frac{i}{2} \sum_{n_r} \text{Res}[W_1(k_x, \omega) \exp(-ik_x x)]_{k_x=k_R} + i \sum_{n_u} \text{Res}[W_1(k_x, \omega) \exp(-ik_x x)]_{k_x=k_u} & x_1 \geq 0 \\ -\frac{i}{2} \sum_{n_r} \text{Res}[W_1(k_x, \omega) \exp(-ik_x x)]_{k_x=k_R} - i \sum_{n_l} \text{Res}[W_1(k_x, \omega) \exp(-ik_x x)]_{k_x=k_l} & x_1 < 0 \end{cases} \quad (19)$$

where k_R represents the real poles of $W_1(k_x, \omega)$; k_u and k_l represent the complex poles of $W_1(k_x, \omega)$ in the upper and lower half of the complex plane, respectively; n_r , n_u , and n_l represent the number of k_R , k_u , and k_l , respectively.

4. VERIFICATION

By setting $S = \text{infinity}$, $r = 0$, $c = 0$, $k_\theta = 0$, $c_\theta = 0$, $\mu = 0$, $\omega = 0$, and neglecting the presence of the vehicle, the beam-foundation-vehicle system becomes an EB beam resting on a Winkler foundation under a moving point load with constant amplitude, which is referred to as the reduced system hereafter. The properties of the beam are $EI = 363.35 \text{ kNm}^2$ and $m = 297.5 \text{ kg/m}$. The stiffness of the foundation is $k = 77.17 \text{ MPa}$. The amplitude of the point load is 70 kN . The critical velocity of the reduced system, defined as $v_{cr} = \sqrt[4]{4EI/m^2}$ (Frýba 1999), is 188.68 m/s . Three velocity cases, 0 , 94.34 , and 226.42 m/s are chosen, which correspond to $\alpha = v/v_{cr} = 0, 0.5$, and 1.2 , respectively. In these cases, the beam deflection is calculated using the present analytical solution and shown in Figure 2, as compared with the closed-form solutions (Frýba 1999). The present solutions of the three cases agree well with the closed-form counterparts. When the loading velocity is lower than the critical velocity, the deflection is a little bit higher than the static deflection. As the loading velocity continues to increase up to a value higher than the critical velocity, more significant deflection along the beam and Doppler effect are observed.

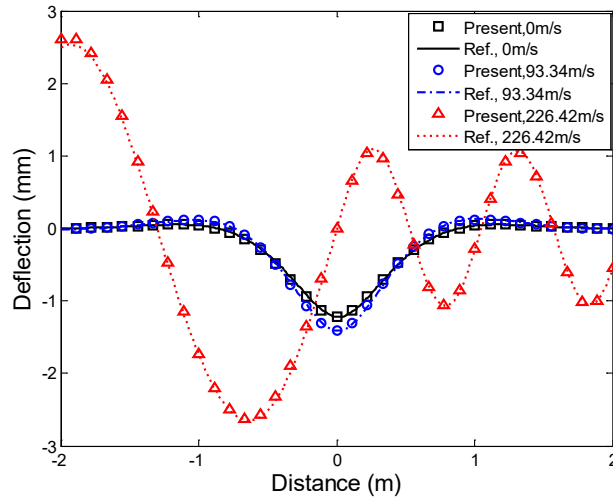


Figure 2. Deflection of an EB beam on a Winkler foundation under a moving point load

5. A NUMERICAL EXAMPLE

In order to investigate the influences of the beam and foundation's properties on the vibration characteristics of the beam, a numerical example is studied in the following sections. The properties of the Timoshenko beam are $S = 100$ MN and $r = 0.1$ m. The properties of the foundation are $c = 10$ kNs/m², $k_\theta = 13.8$ MN, $c_\theta = 5520$ Ns, and $\mu = 25$ kNs (Rezvani and Khorramabadi 2009). The properties of the vehicle are $m_s = 8900$ kg, $m_u = 1100$ kg, $c_s = 40$ kNs/m, $c_t = 4$ kNs/m, $k_s = 2$ MN/m, and $k_t = 3.5$ MN/m (Cebon 1999); and the amplitude of the surface irregularity $U_r = 0.01$ m. Other parameters, such as m , k , and EI , are the same as Section 4. Note that the critical frequency $\omega_{cr} = \sqrt{k/m}$ of the reduced system is 81.06 Hz (Frýba 1999), and two critical frequencies regarding vehicle body and tyre are 1.89 and 11.35 Hz, respectively (Cebon 1999).

229

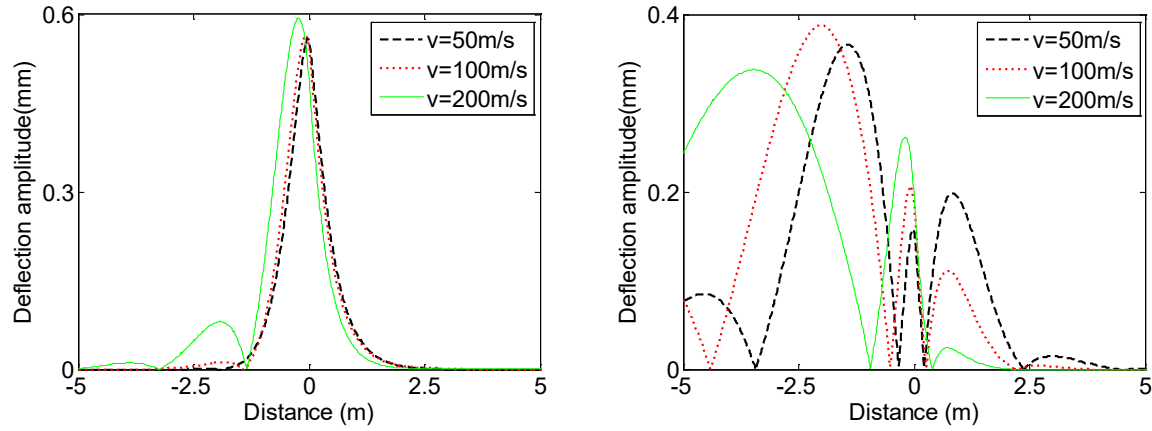
230 In the following sections, the deflected shape versus loading velocity is first studied, followed by
231 the investigation of the influence of beam and foundation's properties on the critical velocity,
232 critical frequency, and their maximum deflections.

233

234 *5.1. Deflected Shape*

235

236 The deflection of the beam is calculated using Eqn 19. Figure 3 shows the results for different
237 load velocities. Two loading frequencies are considered: one is 20 Hz, higher than two critical
238 frequencies of the vehicle but lower than the critical frequency of the reduced system; the other
239 is 100 Hz, higher than all three critical frequencies. The deflected shapes are not symmetric
240 because the vehicular load is moving and the damping of the system is considered. The position
241 of the maximum deflection lags behind the load center, and this lag becomes larger as the vehicle
242 velocity increases. These observations are consistent with the findings by Kim (1996) and Luo *et*
243 *al.* (2015). When the load frequency is 20 Hz, the maximum deflection increases slightly as the
244 load velocity increases; and more fluctuations can be observed behind the load but no fluctuation
245 appears ahead of the load. When the load frequency is 100 Hz, the deflected shapes spread more
246 widely and multiple peaks appear. In particular, the peaks in front of the load decrease as the
247 load velocity increases, while peaks behind the load, the maximum deflection, are case-
248 dependent and will be detailed studied in the following sections.



(a) $f = 20$ Hz

(b) $f = 100$ Hz

Figure 3. Deflection shape of the beam for different load velocities

5.2. Critical Velocity and Maximum Deflection

The maximum deflection of the beam is not only affected by the loading velocity and frequency, but also by the beam and foundation's properties. The relationship between the beam's maximum deflection and load velocity for various beam properties is shown in Figure 4. Generally as the load velocity increases, the maximum deflection increases and then decreases after reaching an extreme value. The velocity corresponding to the extreme value of deflection is referred to as critical velocity. The critical velocity is not obvious in most of cases, which differs from the case of a beam on a Kevin foundation (Kim 2005; Kim and Cho 2006). This is mainly because of an extra viscous shear layer of the Pasternak foundation.

When the load frequency is 20 Hz (see Figure 4a), the critical velocity decreases dramatically as the radius of gyration increases, but the corresponding maximum deflection increases. As the shear rigidity increases, the critical velocity increases, but its corresponding maximum deflection decreases. When the load frequency is 100 Hz (see Figure 4b), both the radius of gyration and the shear rigidity almost have no influence on the critical velocity, while its corresponding maximum deflection increases when the radius of gyration increases.

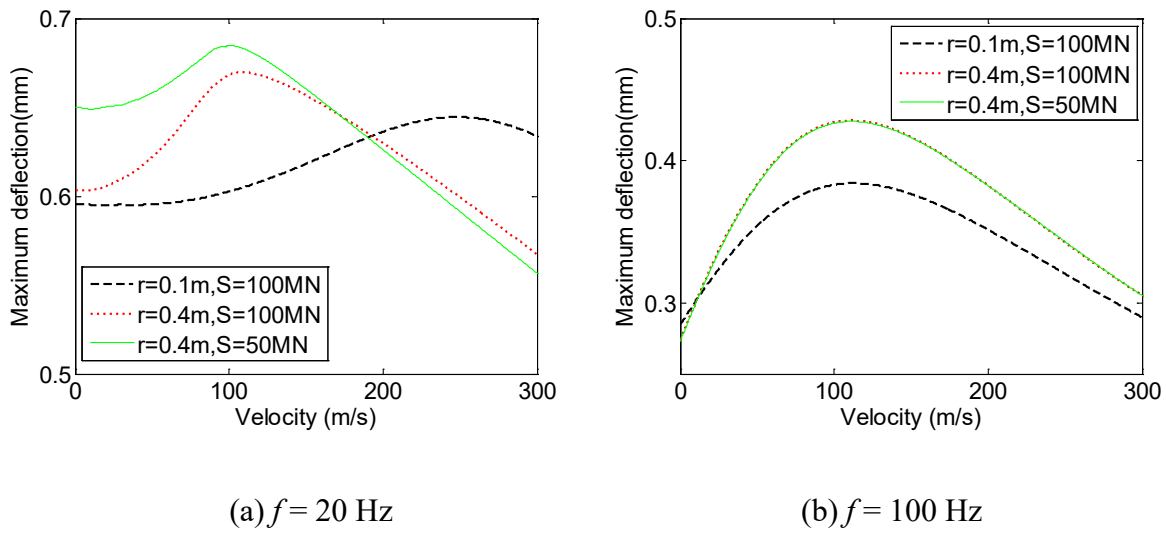


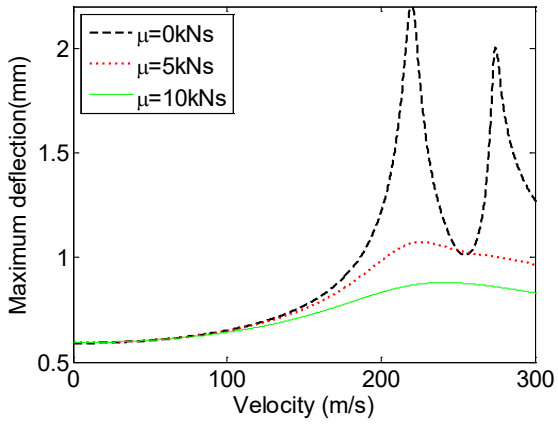
Figure 4. Maximum deflection versus vehicle velocity for different radii of gyration and shear rigidities of the beam

Figures 5a and 5b present the relationship between the maximum deflection of the beam for different shear viscosity coefficients of the foundation, when the load frequencies are 20 Hz and 100 Hz, respectively. In the former case, if no shear viscosity exists, two critical velocities can be clearly observed, which have also been observed by Kim and Roeset (2003). These two peaks almost vanish when the shear viscosity is considered. The maximum deflection decreases as the

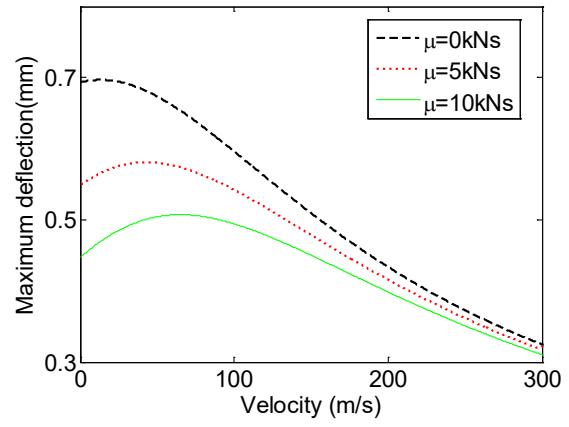
shear viscosity increases. This decrease is more significant at the higher vehicle velocity. When the load frequency is 100 Hz, the critical velocity is rather small (less than 100 m/s), as compared with the 20 Hz counterpart. As the shear viscosity increases, the critical velocity increases, but its maximal deflection decreases.

The effects of the rocking stiffness on the critical velocity and maximum deflection are shown in Figures 5c and 5d, respectively. When the load frequency is 20 Hz, the critical velocity is difficult to identify. The maximum deflection decreases as the velocity increases for a relatively small rocking stiffness (say 5 MN). For a larger value ($k_\theta = 10$ MN), the deflection is almost constant regardless of the velocity. For the case of 100 Hz load frequency, one critical velocity can be found. The corresponding maximum deflection decreases as the rocking stiffness increases.

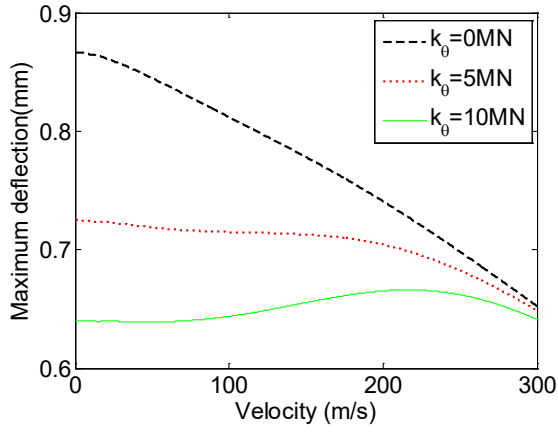
Figures 5e and 5f illustrate the relationship between the maximum deflection and vehicle velocity for various normal stiffness coefficients of the foundation. At 20 Hz load frequency, one critical velocity can still be found. Its value is essentially identical (about 240 m/s) for all three cases, but the corresponding maximum deflection increase significantly as the normal stiffness decreases. In other words, the variation of the normal stiffness seems only affect the amplitude of the maximum deflection. At 100 Hz load frequency, the critical velocity about 150 m/s, much lower than the 20 Hz counterpart. As the normal stiffness increases, this critical velocity increases, whereas its corresponding maximum deflection decreases.



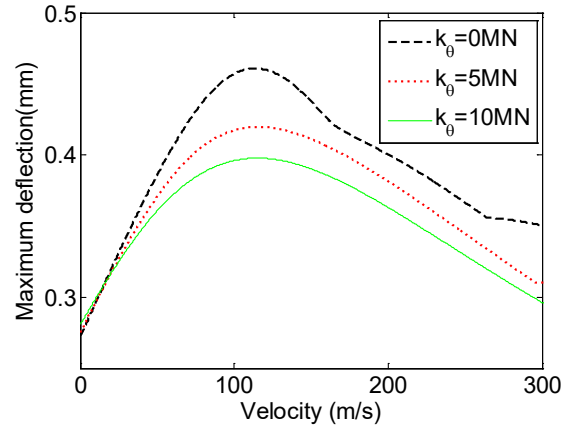
(a) $f = 20$ Hz



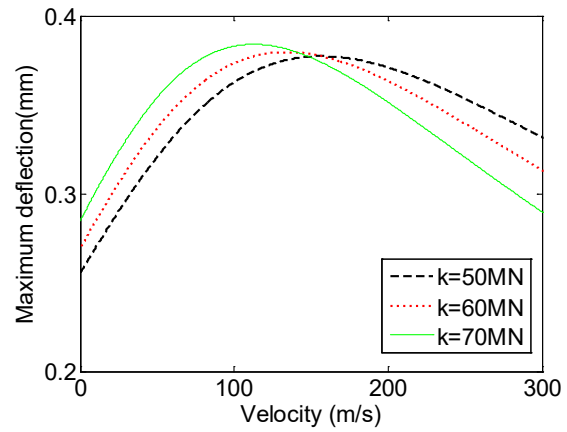
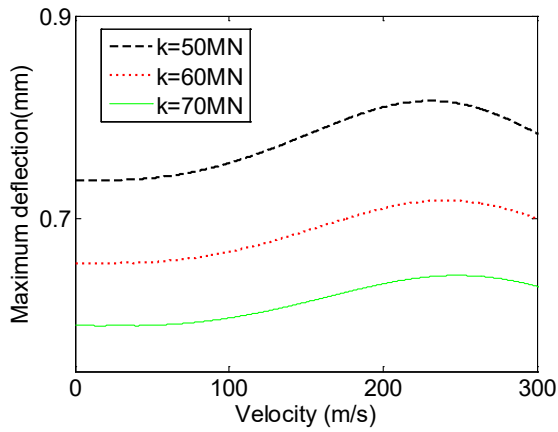
(b) $f = 100$ Hz



(c) $f = 20$ Hz



(d) $f = 100$ Hz



(e) $f = 20$ Hz

(f) $f = 100$ Hz

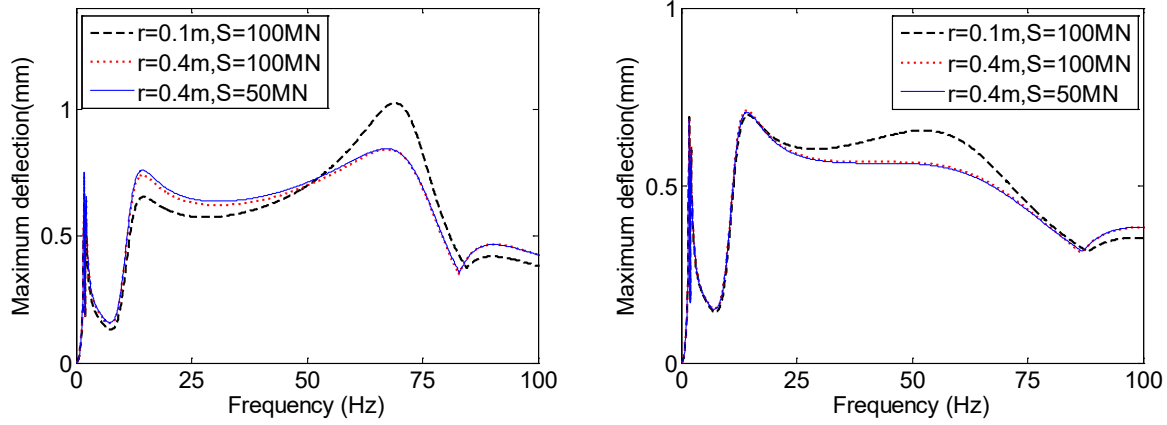
Figure 5. Maximum deflection versus vehicle velocity for different coefficients of the shear viscosity, rocking stiffness, and normal stiffness of the foundation

5.3. Critical Frequency and Maximum Deflection

The effects of the beam and foundation's properties on the critical frequency and maximum deflection are investigated in this section. Two representative vehicle velocities, 100 m/s and 200 m/s, are chosen. The former is lower than the critical velocity of the reduced system; and the latter is higher. Similar the definition of the critical velocity, the frequency corresponding to the local maximum in the curve of maximum deflection versus frequency is regarded as a critical frequency.

Figure 6 shows the maximum deflection versus the load frequency for different radii of gyration and shear rigidities of the beam. Four critical frequencies can be generally observed: the first two are associated with motions of the vehicle body and tyre; and the other two are associated with beam vibrations. The increase of the shear rigidity results in a very small decrease of the maximum deflection, while four critical frequencies are almost not affected. The increase of the radius of gyration, subsequently increasing the stiffness of the beam, does not necessarily result in smaller maximum deflection. Examples can be found in Figure 4b, and the regions 20 – 50 Hz and 85 – 100 Hz of Figure 6a, and the region 85 – 100 Hz of Figure 6b. That is because the

increase of the radius of gyration also decrease the third and fourth critical frequencies, which in turn affect the variation of the maximum deflection curve.

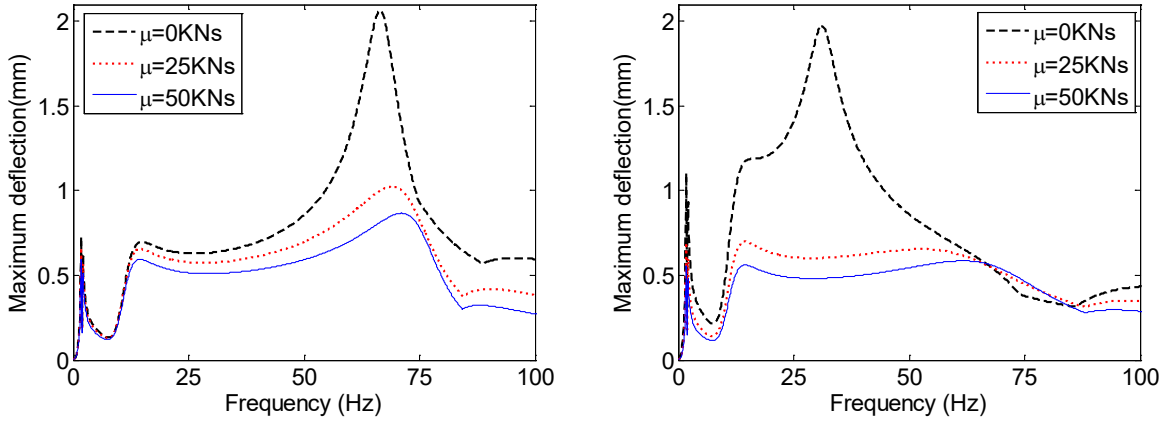


(a) $v = 100$ m/s

(b) $v = 200$ m/s

Figure 6. Maximum deflection versus vehicle frequency for different radii of gyration and shear rigidities of the beam

The effects of the shear viscosity coefficient of the foundation on the critical frequency and maximum deflection are shown in Figure 7. The maximum deflections at all frequencies decrease as the shear viscosity coefficient increases. When no shear viscosity is considered, the sharp peak corresponding to the third critical frequency appears. This peak is almost vanished at a higher shear viscosity in Figure 7b. As the shear viscosity increases, the third critical frequency increases while the fourth one decreases. As expected, the first two regarding vehicle motions are not affected by the shear viscosity.



(a) $v = 100 \text{ m/s}$

(b) $v = 200 \text{ m/s}$

Figure 7. Maximum deflection versus vehicle frequency for different shear viscosity coefficients of the foundation

Figure 8 shows the effects of the rocking stiffness and normal stiffness of the foundation on the maximum deflection and critical frequency when the vehicle velocity is 200 m/s. Generally, the increase of rocking stiffness or normal stiffness leads to a smaller maximum deflection. Some exceptions can also be found in the region of 0 – 100 m/s in Figure 5f, and the region of 50 – 60 Hz in Figure 8a, and the region of 50 – 75 Hz in Figure 8b. That is because the variation of the rocking stiffness or normal stiffness affects both the critical velocity and the last two critical frequencies, which in turn influence the curves of the maximum deflection. Although the first two critical frequencies remain the same, the third one increases as the rocking stiffness or as the normal stiffness increases, and the fourth one also increase as the rocking stiffness increases or as the normal stiffness decreases.

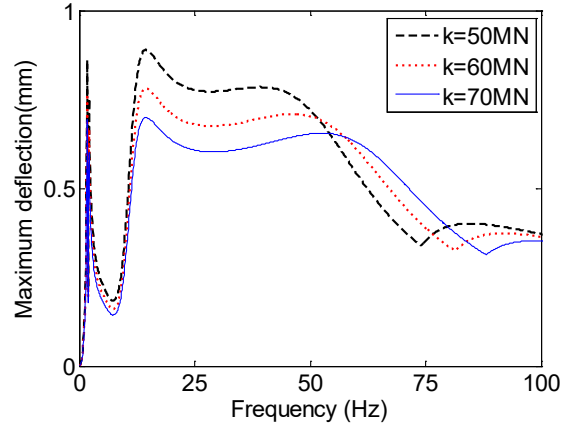
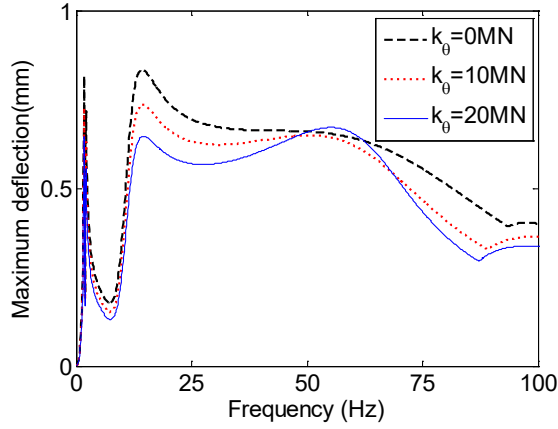


Figure 8. Maximum deflection versus vehicle frequency for different coefficients of the (a) rocking stiffness; and (b) normal stiffness of the foundation when $v = 200$ m/s

6. CONCLUSIONS

The vibration of an infinite Timoshenko beam on a Pasternak foundation subjected to a concentrated vehicular load has been analytically investigated. A quarter car and harmonic irregularity road are considered in calculating the vehicular load. The analytical formulae are validated by comparison with the existed solution of an EB beam on a Winkler foundation. A numerical example is used for parametric study of the beam's vibration. Based on the analytical results, the following conclusions can be drawn:

- (1) The deflected shape of the beam is not sensitive to the load velocity when the load frequency is relatively low as compared with the critical frequencies of the system, while the deflected shape spreads widely and multiple peaks appear when the load frequency is high.

(2) The critical velocity is not obvious, mainly due to the extra viscous shear layer of the Pasternak foundation. When the load frequency is low, the critical velocity decreases as the radius of gyration increases or as the shear rigidity decreases; while the critical velocity is insensitive to both properties when the load frequency is high. The influence of foundation properties on the critical velocity is rather complicated, and the maximum deflection decreases as the increase of the shear viscosity, rocking stiffness, and normal stiffness (only at a low frequency).

(3) Four critical frequencies can be observed in the deflection versus frequency curve. The first two, which are associated with motions of vehicle body and tyre, are constant regardless of the variations of the beam and the foundation's properties. The third critical frequency increases as the increase of the shear viscosity, rocking stiffness, and normal stiffness, or as the decrease of the radius of gyration. The fourth critical frequency increases as the increase of the normal stiffness, or as the decrease of the radius of gyration, shear viscosity, and rocking stiffness. Both values of the critical velocity and critical frequency affect the maximum deflection, and lead to some exceptions in the curves against the beam and the foundation's properties.

ACKNOWLEDGEMENT

This work was supported by The Hong Kong Polytechnic University (Project Nos. G-YN95 and G-YBC7). The first author is thankful to the Research Grants Council of the Hong Kong Special Administrative Region for the Hong Kong PhD Fellowship award.

395

396 **APPENDIX**

397

398 $C_1 = EI - mr^2 v^2$ $C_2 = v(2mr^2 \omega - ic_\theta)$

399 $C_3 = k_\theta + S - mr^2 \omega^2 + ic_\theta \omega$ $C_4 = -iv\mu C_1$

400 $C_5 = C_1 D_1 - \mu v^2(c_\theta + 2imr^2 \omega)$ $C_6 = -ivC_1 D_2 + C_2 D_1 - iv\mu C_3$

401 $C_7 = C_3 D_1 + C_1 D_3 - S^2 - ivC_2 D_2$ $C_8 = C_2 D_3 - ivC_3 D_2$

402 $C_9 = C_3 D_3$ $D_1 = S - mv^2 + i\mu \omega$

403 $D_2 = c + 2im\omega$ $D_3 = k + i\omega c - m\omega^2$

404

405

REFERENCES

- Ahmadian, M.T., Jafari-Talookolaei, R.A. and Esmailzadeh, E. (2008). "Dynamics of a laminated composite beam on Pasternak-viscoelastic foundation subjected to a moving oscillator", *Journal of Vibration and Control*, Vol. 14, No. 6, pp. 807-830.
- Çalım, F.F. (2009). "Dynamic analysis of beams on viscoelastic foundation", *European Journal of Mechanics-A/Solids*, Vol. 28, No. 3, pp. 469-476.
- Cebon, D. (1999), *Handbook of Vehicle-Road Interaction*, Taylor & Francis.
- Frýba, L. (1999), *Vibration of Solids and Structures under Moving Loads*, Thomas Telford, London, UK.
- Gao, Q.F., Wang, Z.L., Koh, C.G., and Chen, C. (2015). "Dynamic load allowances corresponding to different responses in various sections of highway bridges to moving vehicular loads", *Advances in Structural Engineering*, Vol. 18, No. 10, pp. 1685-1701.
- Hao, H., and Ang, T.C. (1998). "Analytical modeling of traffic-induced ground vibrations", *Journal of Engineering Mechanics-ASCE*, Vol. 124, No. 8, pp. 921-928.
- Hunt, H.E.M. (1991). "Modeling of road vehicles for calculation of traffic-induced ground vibration as a random process", *Journal of Sound and Vibration*, Vol. 144, No. 1, pp. 41-51.
- Ju, S.H. (2009). "Finite element investigation of traffic induced vibrations", *Journal of Sound and Vibration*, Vol. 321, No. 3-5, pp. 837-853.
- Kargarnovin, M.H., and Younesian, D. (2004). "Dynamics of Timoshenko beams on Pasternak foundation under moving load", *Mechanics Research Communications*, Vol. 31, No. 6, pp.713-723.
- Kenney, J.T. (1954). "Steady-state vibrations of beam on elastic foundation for moving load", *Journal of Applied Mechanics - ASME*, Vol. 21, No. 4, pp. 359-364.
- Kim, S.M. (1996). *Dynamic Response of Pavement Systems to Moving Loads*, PhD Thesis, University of Texas at Austin, Texas, USA.
- Kim, S.M. (2005). "Stability and dynamic response of Rayleigh beam-columns on an elastic foundation under moving loads of constant amplitude and harmonic variation", *Engineering Structures*, Vol. 27, No. 6, pp. 869-880.
- Kim, S.M., and Cho, Y.H. (2006). "Vibration and dynamic buckling of shear beam-columns on elastic foundation under moving harmonic loads", *International Journal of Solids and Structures*, Vol. 43, No. 3-4, pp. 393-412.
- Kim, S.M., and Roesset, J.M. (2003). "Dynamic response of a beam on a frequency-independent damped elastic foundation to moving load", *Canadian Journal of Civil Engineering*, Vol. 30, No. 2, pp. 460-467.

- 442 Lombaert, G., Degrande, G. and Clouteau, D. (2000). "Numerical modelling of free field traffic-
443 induced vibrations", *Soil Dynamics and Earthquake Engineering*, Vol. 19, No. 7, pp. 473-488.
- 444 Luo, W.L., Xia, Y. and Weng, S. (2015). "Vibration of Timoshenko beam on hysteretically
445 damped elastic foundation subjected to moving load", *SCIENCE CHINA Physics, Mechanics &
446 Astronomy*, Vol. 58, No. 6, pp. 1-9.
- 447 Luo, W. L., Xia, Y., and Zhou, X.Q. (2016). "A closed-form solution to a viscoelastically
448 supported Timoshenko beam under harmonic line load", *Journal of Sound and Vibration*,
449 Vol.369, pp, 109-118.
- 450 Mathews, P.M. (1958). "Vibrations of a beam on elastic foundation", *ZAMM-Journal of Applied
451 Mathematics and Mechanics*, Vol. 38, No. 3-4, pp. 105-115.
- 452 Metrikine, A.V., and Dieterman, H.A. (1997). "Instability of vibrations of a mass moving
453 uniformly along an axially compressed beam on a viscoelastic foundation", *Journal of Sound
454 and Vibration*, Vol. 201, No. 5, pp. 567-576.
- 455 Rezvani, M.J., and Khorramabadi, K.M. (2009). "Dynamic analysis of a composite beam
456 subjected to a moving load", *Proceedings of the Institution of Mechanical Engineers, Part C:
457 Journal of Mechanical Engineering Science*, Vol. 223, No. 7, pp. 1543-1554.
- 458 Sun, L. (2001). "A closed-form solution of a Bernoulli-Euler beam on a viscoelastic foundation
459 under harmonic line loads", *Journal of Sound and Vibration*, Vol. 242, No. 4, pp. 619-627.
- 460 Sun, L. (2002). "A closed-form solution of beam on viscoelastic subgrade subjected to moving
461 loads", *Computers & Structures*, Vol. 80, No. 1, pp. 1-8.
- 462 Sun, L. (2003). "An explicit representation of steady state response of a beam on an elastic
463 foundation to moving harmonic line loads", *International Journal for Numerical and Analytical
464 Methods in Geomechanics*, Vol. 27, No. 1, pp. 69-84.
- 465 Verichev, S.N., and Metrikine, A.V. (2002). "Instability of a bogie moving on a flexibly
466 supported Timoshenko beam", *Journal of Sound and Vibration*, Vol. 253, No. 3, pp. 653-668.
- 467 Wolfert, A.R.M., Dieterman, H.A., and Metrikine, A.V. (1998), "Stability of vibrations of two
468 oscillators moving uniformly along a beam on a viscoelastic foundation", *Journal of Sound and
469 Vibration*, Vol. 211, No. 5, pp. 829-842.
- 470 Yin, X.F., Liu, Y., Deng, L., and Cai, C.S. (2016), "Impact factors of bridges in service under
471 stochastic traffic flow and road surface progressive deterioration", *Advances in Structural
472 Engineering*, Vol. 19, No. 1, pp. 38-52.

473